Routes to chaos in a semiconductor laser subject to phase-conjugate optical feedback

Bernd Krauskopf and Kirk Green

Engineering Mathematics, University of Bristol, Bristol BS8 1TR, UK

ABSTRACT

A semiconductor laser subject to phase-conjugate optical feedback can be described by rate equations, which are mathematically delay differential equations (DDEs) with an infinite dimensional phase space. This is why, from the theoretical point of view, this system was only studied by numerical simulation up to now. We employ new numerical techniques for DDEs, namely the continuation of periodic orbits and the computation of unstable manifolds, to study bifurcations and routes to chaos in the system. Specifically we compute 1D unstable manifolds of a saddle-type periodic orbit as intersection curves in a suitable Poincaré section. We are able to explain in detail a transition to chaos as the feedback strength is increased, namely the break-up of a torus and a sudden transition to chaos via a boundary crisis. This allows us to make statements on properties of the ensuing chaotic attractor, such as its dimensionality. Information of this sort is important for applications of chaotic laser signals, for example, in communication schemes.

Keywords: Semiconductor laser, phase-conjugate optical feedback, routes to chaos, bifurcation analysis

1. INTRODUCTION

Our object of study is a semiconductor laser with phase-conjugate feedback (PCF), due to external reflection from a phase-conjugating mirror (PCM). This system, also called the PCF laser, is schematically shown in Fig. 1. Phase-conjugate feedback is interesting as it produces a reflected wave that is wave-front inverted, with the angle of incidence of the wave being equal to the angle of reflection, so that the setup is 'self-aligning'. Furthermore, distortions in the external cavity are undone over one external round-trip. Applications of PCF include mode locking[1] and phase locking, where PCF has been shown to reduce the laser noise considerably.[2–4]

The PCF laser is an example of the technologically important class of laser systems with feedback,[5] which can be modelled with delay differential equations (DDEs).[6,7] Other such lasers systems include lasers subject to conventional optical feedback (COF) from an external mirror,[8,9] mutually coupled lasers with delay,[10] and lasers with opto-electronic feedback.[11] In many applications chaotic output is unwanted, and expensive optical isolators need to be used. However, recently there has been considerable interest in the controlled production of chaotic optical laser output for use in chaotic communication schemes.[12,13] In general, an understanding of the dynamics of lasers with delay can lead to new uses and better control of lasers.

The PCF laser has been shown to exhibit a wealth of dynamics, including stable periodic operation, quasiperiodic motion and chaos.[4,14] Transitions to chaos were studied by simulation, with a combination of bifurcation diagrams and phase-plots in Ref. [14]. In this paper we address the question: what are the *global dynamics* underlying these transitions? To this end, we use numerical tools that go beyond simulation, namely the continuation of saddle-type periodic orbits and the computation of their unstable manifolds. Specifically, we show how an invariant torus breaks up and disappears in an attractor crisis, leading to the sudden onset of chaotic laser output.

E-mail addresses: B.Krauskopf@bristol.ac.uk, Kirk.Green@bristol.ac.uk

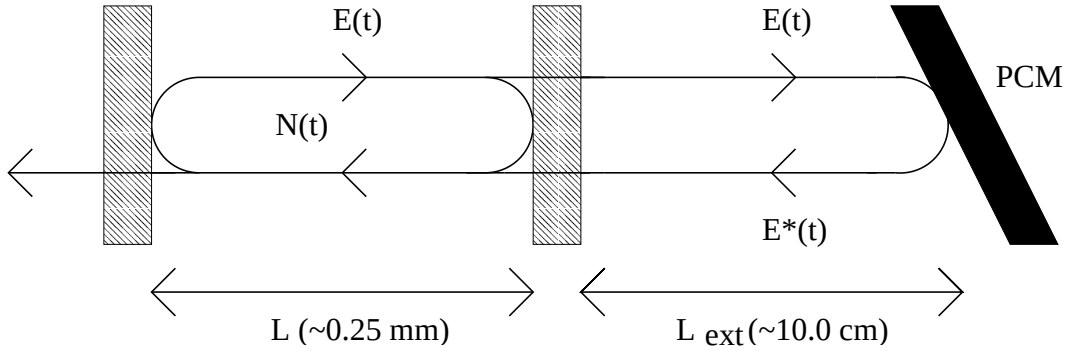

Figure 1: Sketch of a semiconductor laser with phase-conjugate feedback.

2. RATE EQUATIONS OF PCF LASER

A single-mode semiconductor laser with instantaneous PCF can be described by the rate equations[14]

$$\frac{dE}{dt} = \frac{1}{2}\left[-i\alpha G_N(N(t)-N_{\rm sol}) + \left(G(t)-\frac{1}{\tau_p}\right)\right]E(t) + \kappa E^*(t-\tau)\exp[i\phi_{\rm PCM}] \quad (1)$$

$$\frac{dN}{dt} = \frac{I}{q} - \frac{N(t)}{\tau_e} - G(t)\,|E(t)|^2 \quad (2)$$

for the evolution of the slowly varying complex electric field $E(t)$ and the population inversion $N(t)$. Here, nonlinear gain is included as $G(t) = G_N(N(t)-N_0)(1-\epsilon P(t))$, where $\epsilon = 3.57\times10^{-8}$ is the nonlinear gain coefficient and $P(t) = |E(t)|^2$ is the intensity. Parameter values are set to realistic values corresponding to a Ga-Al-As semiconductor laser, as set out in detail in Refs. [4, 14, 15]. The feedback term in Eqs. (1,2) involves the feedback rate κ and the external cavity round-trip time τ, which was fixed at $\tau = 2/3\,$ns. Together they form the dimensionless bifurcation parameter $\kappa\tau$.

Equations (1,2) are symmetric under the transformation $E \to -E$, which is a rotation over π of the complex E-plane corresponding to a phase-shift by π of the phase of the laser light. As a consequence, every attractor (or other invariant set) is either symmetric or has a symmetric counterpart. This symmetry allows the possibility of symmetry-breaking and symmetry-restoring bifurcations,[14, 16] and also implies restrictions on the types of bifurcations of periodic orbits; see Ref. [15] for more details.

Equations (1,2) are a system of DDEs with the infinite-dimensional *phase space* of continuous function on the time interval $[-\tau, 0]$ with values in (E, N)-space; see Refs. [15, 17]. A *state* q of Eqs. (1,2) is of the form

$$q \equiv \{\,(E(t), N(t)) \mid t \in [-\tau, 0]\,\}$$

where we call $q(0)$ the *head-point* of q and $\{q(t) \mid t \in [-\tau, 0)\}$ its *history*. A state q, that is, knowledge of (E, N) over the entire interval $[-\tau, 0]$, is an initial condition and uniquely determines the dynamics for $t \in [-\tau, \infty)$. One usually plots trajectories of Eqs. (1,2) in (E, N)-space, which is also called the *physical space*.

An *equilibrium* (or steady state) is a solution $(E(t), N(t)) = (E_0, N_0)$ for all $t \in [-\tau, \infty)$ and fixed (E_0, N_0). The main object of study in this paper are *periodic solutions* along which any state q is mapped to itself after integration of Eqs. (1,2) over some fixed period T. The stability of a periodic solution is determined by its Floquet multipliers, which are the solutions of a transcendental eigenvalue problem given by the linearisation of Eqs. (1,2) along the periodic orbit. There are infinitely many Floquet multipliers, but only finitely many unstable ones (outside the unit circle). When a Floquet multiplier crosses the unit circle a bifurcation occurs, namely, a saddle-node bifurcation of limit cycles when a real Floquet multiplier crosses at $+1$, a period-doubling bifurcation when a real Floquet multiplier crosses at -1, and a torus (or Neimark-Sacker) bifurcation when a pair of complex Floquet multipliers cross the unit circle.

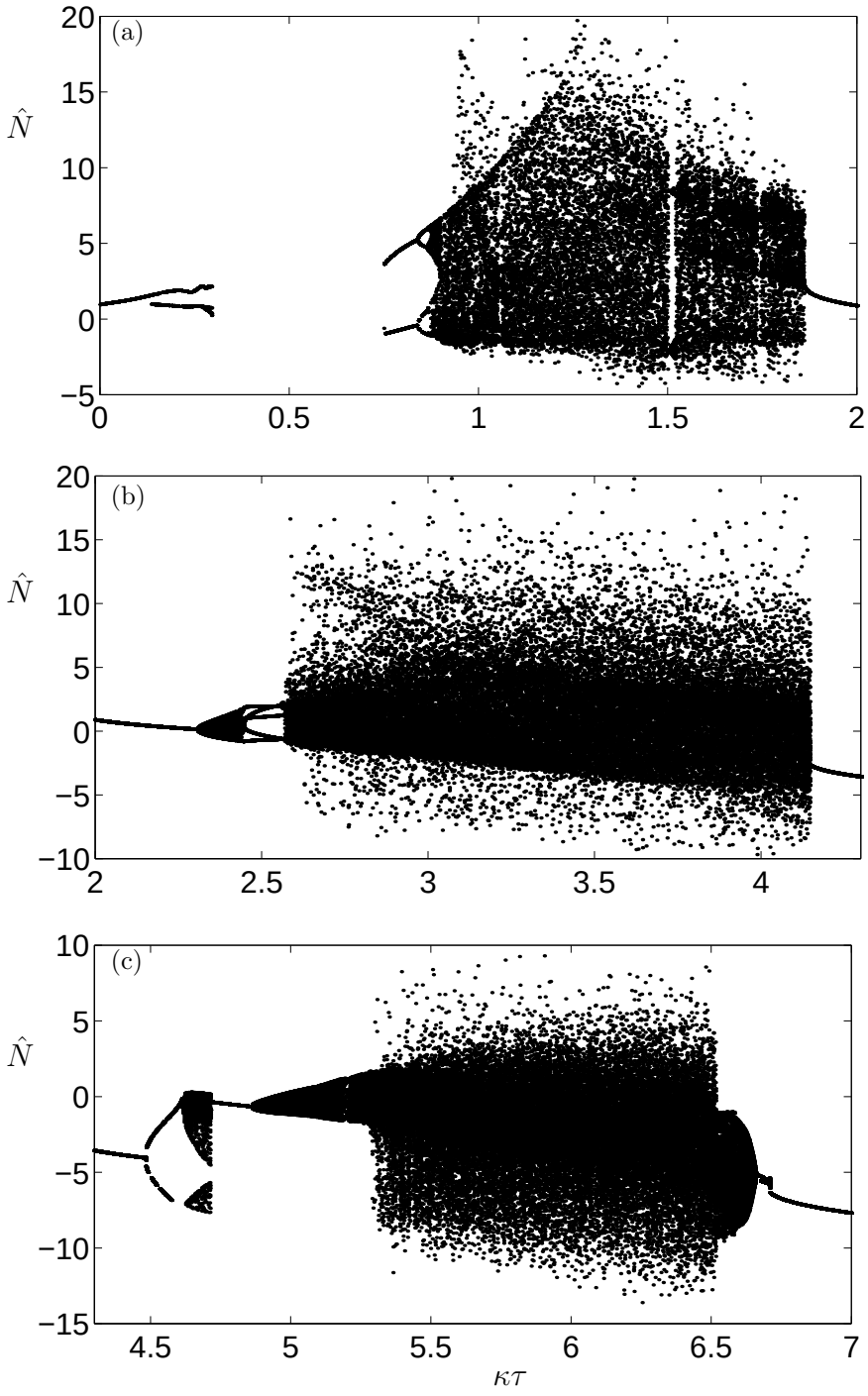

Figure 2. The bifurcation diagram for $\kappa\tau \in [0.0, 7.0]$, obtained by numerical simulation, shows stable periodic operation interspersed with three 'bubbles', in (a)-(c), of more complicated dynamics.

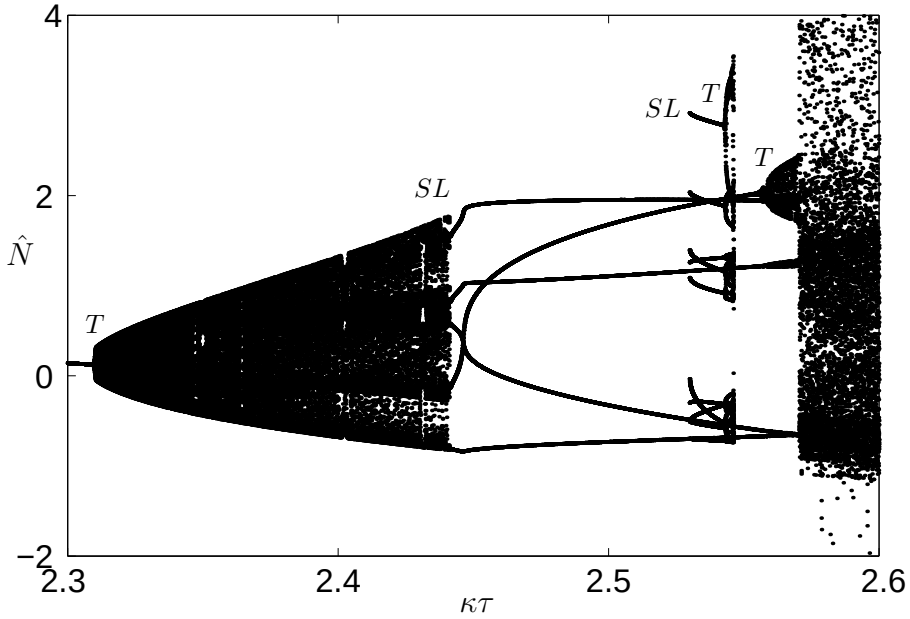

Figure 3. The bifurcation diagram for $\kappa\tau \in [2.3, 2.6]$, enlarging the transition to chaos at the beginning of the second 'bubble' in Fig. 2 (b). The extra attractors for $\kappa\tau \in [2.530, 2.546]$ can only be found with continuation techniques; see Fig. 4 and the text.

3. THE BIFURCATION DIAGRAM

The general picture of the dynamics of the PCF laser is that, as $\kappa\tau$ is changed, the laser produces stable periodic output interspersed with 'bubbles' of more complicated dynamics, which for the most part are chaotic.[4,14] This can be seen in the bifurcation diagram in Fig. 2 for $\kappa\tau \in [0.0, 7.0]$, which was obtained as follows. For each value of $\kappa\tau$, we integrated Eqs. (1,2) with an Adams-Bashford method,[17] where we started with an initial condition on the attractor for the previous value of $\kappa\tau$ and let transients die away. Then we plotted $\hat{N} = (N/N_{sol} - 1) \times 10^3$ whenever the intensity crossed its average value in the increasing direction. No points indicate a solution phase locked to that of the solitary laser, a small number of points correspond to a periodic solution, while a large number of points indicate quasiperiodic or chaotic dynamics.

Several transitions to chaos can be seen. At the beginning of the 'first bubble', in Fig. 2 (a), one recognizes period-doubling to chaos; see also Ref. [18]. There are other transitions into and out of bubbles. We mention here an intermittent transition due to a saddle-node bifurcation of a limit cycle[14] at the end of bubbles one and two and several instances of what appear to be transitions involving quasiperiodic motion and the break-up of tori, both at the beginning of bubble two and at the end of bubble three.

We now consider a transition involving the break-up of a torus in detail. To this end, we focus on the exact nature of the transition to chaos at the beginning of the 'second bubble', in Fig. 2 (b), in the range of $\kappa\tau \in [2.3, 2.6]$. The bifurcation diagram of this transition is enlarged in Fig. 3 and suggests the following scenario. The periodic solution at $\kappa\tau = 2.300$, corresponding to oscillations of the power, loses stability in a torus bifurcation T at $\kappa\tau \approx 2.307$. The ensuing dynamics is quasiperiodic and takes place on an attracting torus; the power oscillations of the torus are now amplitude modulated by a second incommensurate frequency. At $\kappa\tau \approx 2.441$ the dynamics on the torus becomes locked to a stable periodic solution in a saddle-node bifurcation of limit cycles SL. The bifurcating periodic orbit makes five loops around the torus, leading to the five branches in Fig. 3. Physically, the laser power oscillates with a basic period, but its amplitude is subject to modulations that repeat after exactly five basic oscillations. This periodic solution undergoes a torus bifurcation T itself at $\kappa\tau \approx 2.556$, resulting in a new torus that winds around the old, large torus like a garden hose. The locked

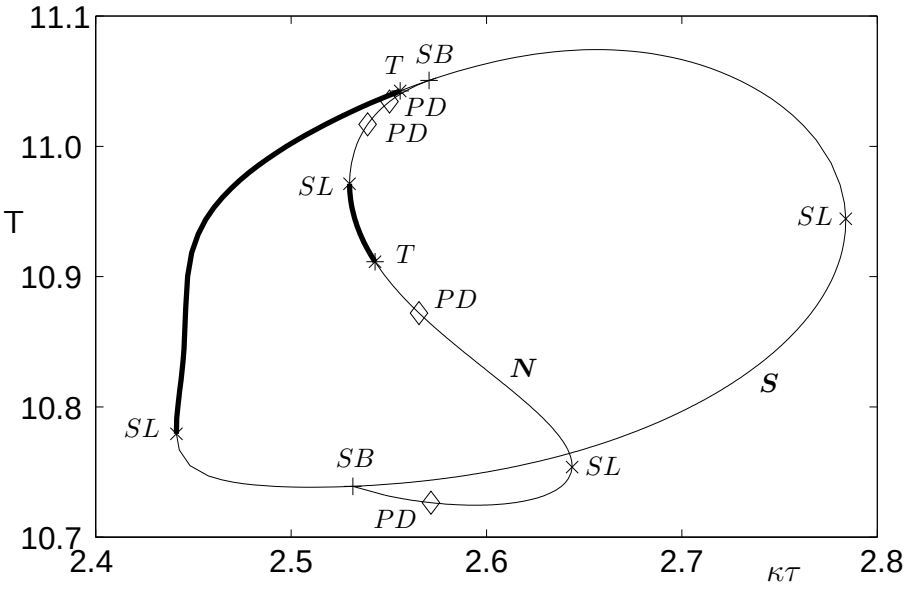

Figure 4: Continuation of periodic orbits for $\kappa\tau \in [2.4, 2.8]$; attracting periodic orbits are boldfaced.

amplitude oscillations are now themselves modulated! In the spectrum we would expect three frequencies, two of which are commensurate. This 'hose-like' torus is destroyed at $\kappa\tau \approx 2.571$ and the dynamics becomes chaotic. We stress that there is no hysteresis in this transition. (The additional attractors in Fig. 3 for $\kappa\tau \in [2.530, 2.546]$ are explained below.)

A similar route to chaos has been observed, by simulation, in a semiconductor laser with COF.[9] The dynamics after the second torus bifurcation was interpreted as quasiperiodic motion with three-frequencies. We remark that, mathematically, we are dealing with a two-torus, involving only two independent frequencies. However, due to the hose-like structure of this torus, one of these two 'mathematical frequencies' corresponds to the old locked solution around the original torus and, hence, it already contains two 'physical frequencies', which are rationally related.

4. CONTINUATION OF UNSTABLE PERIODIC ORBITS

In order to find the mechanism involved in the sudden transition from the attracting torus to a much larger chaotic attractor, we need to use new tools for DDEs that go beyond simulation of Eqs. (1,2). The first step is to find the unstable periodic orbit on the locked torus. This can be done with the package DDE-BIFTOOL,[19] consisting of Matlab routines for the bifurcation analysis of steady states and periodic solutions of DDEs. We used DDE-BIFTOOL to find and follow the periodic orbits responsible for the locking on the torus, irrespective of their stability. By computing Floquet multipliers, DDE-BIFTOOL also detects (codimension-one) bifurcations. It is possible to compute bifurcating branches of periodic orbits from detected bifurcation points. Because of the symmetry, a Floquet multiplier crossing +1 may correspond to a symmetry-breaking bifurcation, and DDE-BIFTOOL was recently extended to allow branch switching at symmetry-breaking bifurcations as well; see Ref. [15] for more details.

In Fig. 4 we plot the period T of periodic orbits against $\kappa\tau$. The computation was started from the stable locked periodic solution on the torus, and attracting solutions are drawn as boldfaced curves, while unstable solutions are thin. Figure 4 shows an oval branch $\boldsymbol{S}$ of symmetric periodic solutions and a branch $\boldsymbol{N}$ of non-symmetric periodic solutions, which is connected to the top and bottom parts of $\boldsymbol{S}$ at symmetry breaking bifurcations SB. The end points of $\boldsymbol{S}$ are saddle-node bifurcations of limit cycles SL.

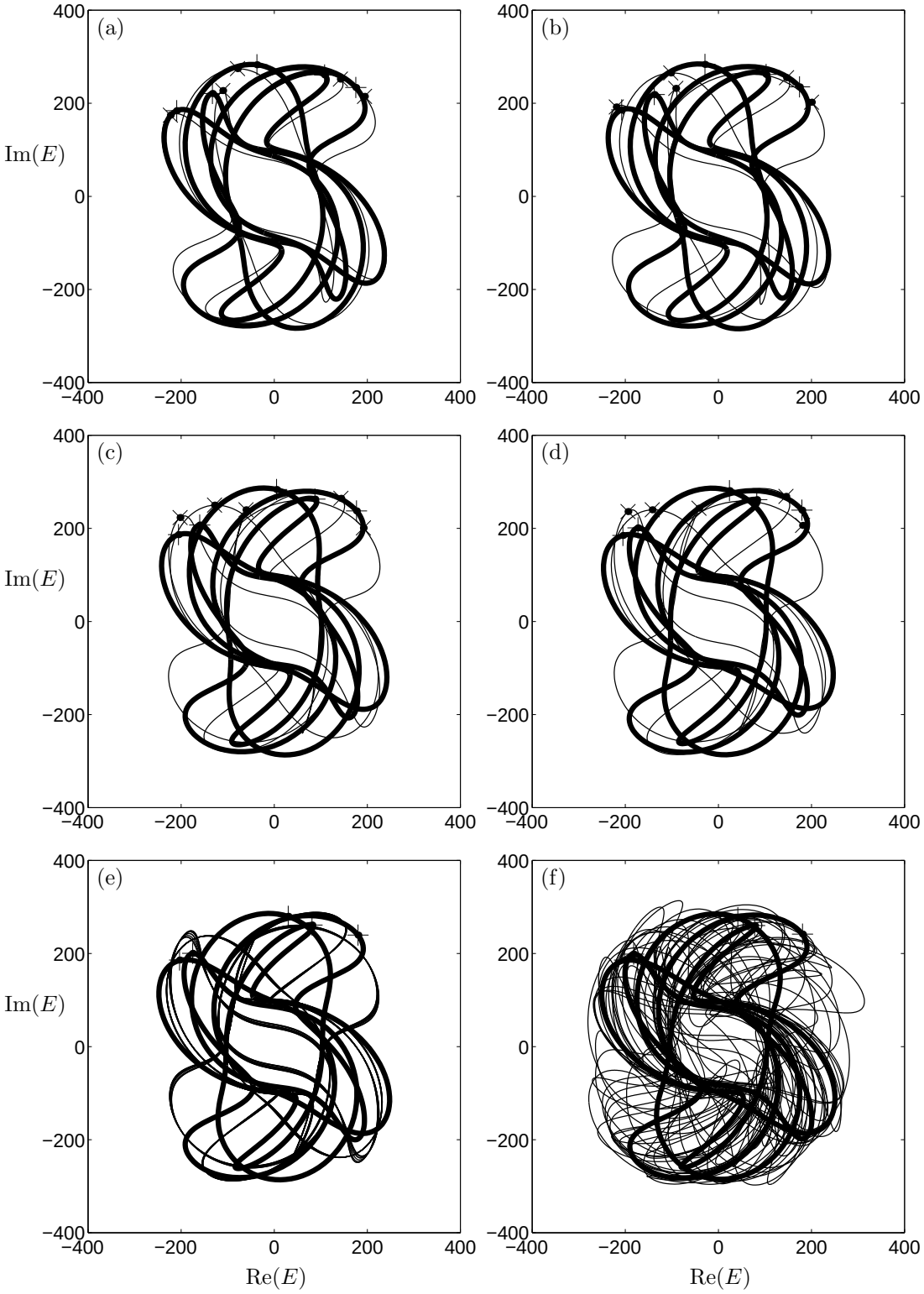

Figure 5. Phase portraits of unstable periodic orbits (boldfaced) together with the respective attractors (thin); from (a) to (f) $\kappa\tau$ takes the values 2.445, 2.450, 2.500, 2.550, 2.5625 and 2.600.

The locked stable solution (boldfaced curve in Fig. 4), lies on the upper part of $\boldsymbol{S}$. It is born at SL for $\kappa\tau \approx 2.441$, marking the onset of locking, and becomes unstable at $\kappa\tau \approx 2.556$ in the torus bifurcation T; compare Fig. 3. The unstable solution exists until $\kappa\tau \approx 2.784$, where it bifurcates with the lower part of $\boldsymbol{S}$ at another point SL. There are two additional bifurcations of unstable solutions on $\boldsymbol{S}$, namely the symmetry-breaking bifurcations SB.

In Fig. 5 are shown the unstable periodic orbits (boldfaced) together with the respective attractors (thin) for increasing values of $\kappa\tau$ from locking to chaos, illustrating in projection to the E-plane the transition we discussed in the previous section. In Fig. 5 (a)-(d) the attractor is a periodic orbit, in Fig. 5 (e) it is the hose-like torus and in Fig. 5 (f) the attractor is in fact chaotic. (We remark that the chaotic dynamics get very close to the origin of the E-plane at irregular moments in time, which correspond to power drop-outs of the laser.) Note that, the saddle periodic orbit (boldfaced) does not change qualitatively throughout the range of $\kappa\tau$ in Fig. 5.

When continuing the branch $\boldsymbol{N}$ from SB at $\kappa\tau \approx 2.532$ on the lower part of $\boldsymbol{S}$, a period-doubling bifurcation PD is detected, from which a period-doubled branch (not shown in Fig. 4) bifurcates. Next, a saddle-node bifurcation of limit cycles SL is detected and then another period-doubling bifurcation PD. At $\kappa\tau \approx 2.543$ a torus bifurcation T leads to a stable solution, indicated by the boldfaced part of $\boldsymbol{N}$. This stable solution becomes unstable at a saddle-node bifurcation of limit cycles SL at $\kappa\tau \approx 2.530$. There are two more period-doubling bifurcations PD along $\boldsymbol{N}$, which are in fact connected by a branch of period-doubled unstable solutions (again not shown in Fig. 4). After this, $\boldsymbol{N}$ joins the upper part of $\boldsymbol{S}$ at the symmetry-breaking bifurcation SB.

By following the bifurcating branch $\boldsymbol{N}$ of initially unstable solutions, we have found values of $\kappa\tau$ for which there exists another stable solution next to the locking on the torus. In other words, we found a bistability. We remark that there is no hysteresis when one follows the main attractor in Fig. 3, because the window of stability on $\boldsymbol{N}$ is connected to $\boldsymbol{S}$ via unstable branches. Consequently, scanning back and forth in the bifurcation diagram, the dynamics is always attracted to the main attractor. This is why this bistability has not been found by simulation. The basin of attraction of this new attractor is quite small, but by using the stable solution obtained with DDE-BIFTOOL as starting data we computed the associated bifurcation diagram and plotted it also in Fig. 3. As found by continuation, a stable periodic orbit is born at $\kappa\tau \approx 2.530$ in a saddle-node bifurcation of limit cycles SL, and then undergoes a torus bifurcation T at $\kappa\tau \approx 2.543$. The dynamics then locks to a periodic solution on the torus, which appears to undergo a period-doubling cascade to a small region of chaos. The chaotic attractor disappears suddenly at $\kappa\tau \approx 2.546$, and the solution jumps to the main attractor of Eqs. (1,2).

5. BREAK-UP OF TORUS

In order to understand the transition to chaos fully, in particular, the sudden change from an attracting torus to a much larger chaotic attractor, we need to investigate what happens to the underlying torus after locking. For this it is not sufficient to use mere simulation, because this will only produce the attractors in Fig. 5. Instead one needs to compute the unstable manifolds of the saddle periodic orbits.

We first need to recall some theory.[6,17] Near a periodic orbit, we define the *Poincaré map* P which maps a state q with head-point in the section $\Sigma = \{N = 7.62 \times 10^8\}$ to $P(q)$, which is again a state with head-point in Σ. The periodic orbit of the DDE corresponds to one (or several) fixed points of the Poincaré map P. The *unstable manifold* $W^u(q)$, of such a saddle fixed point q, is the set of all states p that can be iterated backwards under P and reach q in the limit. When exactly one Floquet multiplier is outside the unit circle, as is the case for the saddle-periodic orbits in Fig. 5, then the *trace* $W^u(q) \cap \Sigma$ is a one-dimensional curve in Σ. Notice, that the trace may have self-intersections, because it is really the projection of the infinite-dimensional object $W^u(q)$ onto a two-dimensional plane.[17] Nevertheless, we still speak of a 1D unstable manifold because there is exactly one unstable direction.

We developed a method that computes the 1D unstable manifold $W^u(q)$ of a saddle fixed point q of a suitable Poincaré map defined by a section Σ. We summarize here briefly how this is done and refer to Ref. [17] for further details. Our method grows the unstable manifold such that the distance of the headpoints in the section Σ is adapted according to the curvature of the trace $W^u(q) \cap \Sigma$. In this way, we achieve the best possible numerical approximation given pre-specified accuracy parameters. As just mentioned, the trace is a smooth

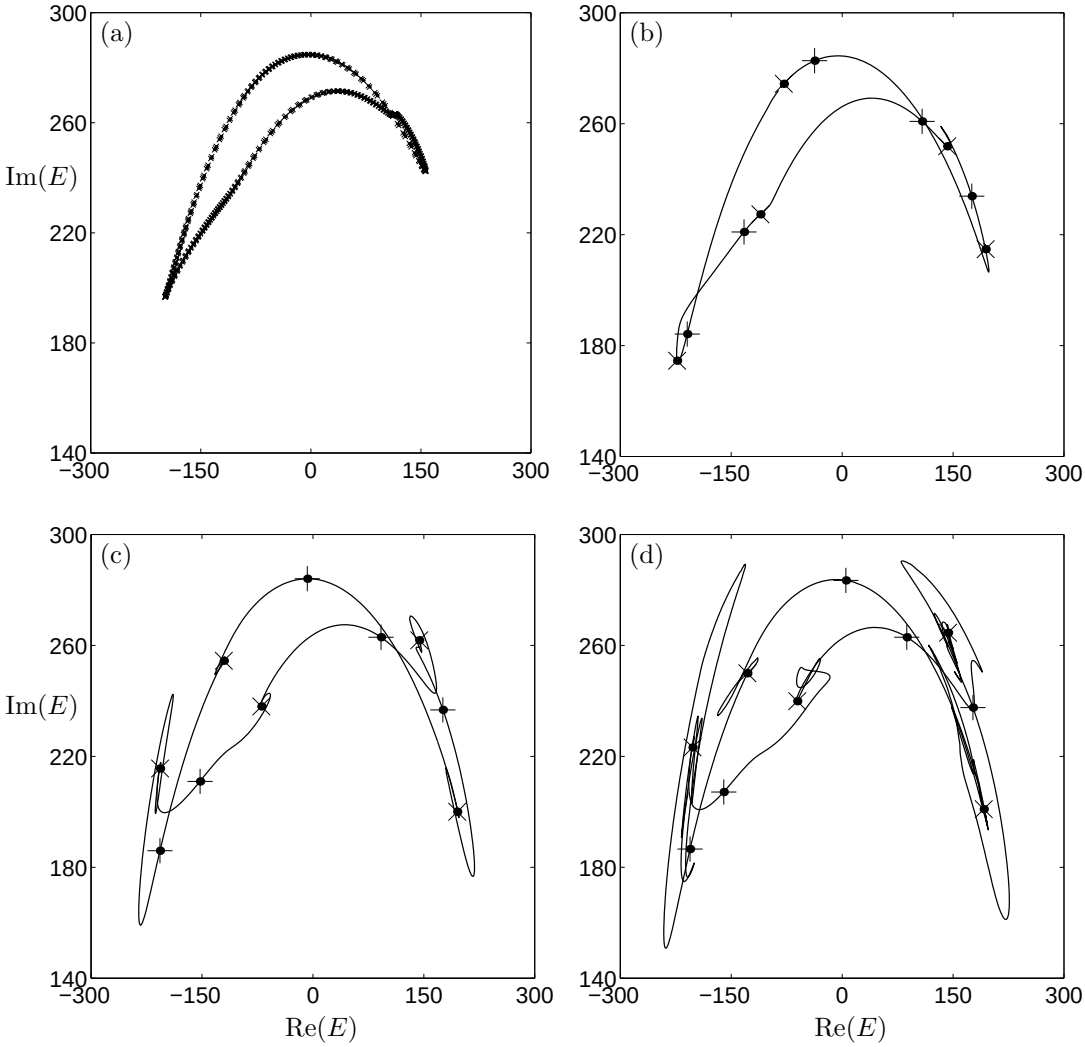

Figure 6. The invariant torus or what is left of it. Panel (a) shows the trace of the quasiperiodic torus for $\kappa\tau = 2.400$ and panels (b)-(d) show the 1D unstable manifolds of the five saddle periodic orbits for $\kappa\tau = 2.450, 2.480, 2.500$, respectively.

1D curve (except at isolated points, where smoothness may be lost due to the projection), so that it can be interpreted in much the same way as a 1D unstable manifold of a planar map.

Computing 1D unstable manifolds, allows us, for the first time in DDEs, to compute certain invariant objects and, in particular, the underlying torus in the locking region. The unstable manifolds in this paper were computed with the accuracy parameters set to the values in Refs. [15, 17].

What happens to the torus is shown in Fig. 6, where we plot the 1D unstable manifolds of the saddle periodic orbits on the lower part of branch $\boldsymbol{S}$ in Fig. 4. They have exactly one unstable Floquet multiplier, that is, their unstable manifolds are indeed one-dimensional. In the Poincaré section Σ, each saddle periodic orbit corresponds to five intersection points, which represent five saddle fixed points of the Poincaré map. The plusses (+) in Fig. 6 mark the five intersection points of the saddle periodic orbit, and the crosses ($\times$) mark those of the corresponding stable periodic orbits. From each saddle point there emanate two branches of the unstable manifold, which converge to neighbouring attracting points. The closure of these branches forms the trace in Σ of the invariant torus, or what is left of it.

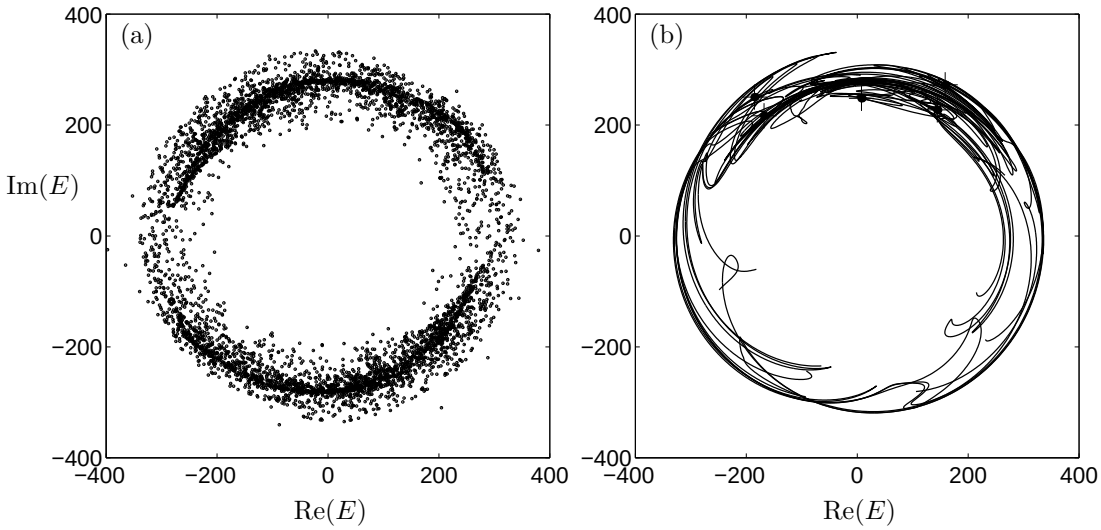

Figure 7: Trace of the chaotic attractor (a) and the 1D unstable manifold (b); $\kappa\tau = 2.700$.

Figure 6 (a) shows the trace of a quasiperiodic torus. When $\kappa\tau$ is increased, the dynamics locks, as is shown Fig. 6 (b). Notice that the locked torus is initially smooth, as one expects immediately after locking. Smoothness is lost when $\kappa\tau$ is increased further, because the manifold starts to spiral into the stable points; see Fig. 6 (c). Physically, this corresponds to damped oscillations as the laser settles down to the periodic solution. As $\kappa\tau$ is increased even further as in Fig. 6 (d), the unstable manifold increasingly folds and stretches. This means that the transients are becoming increasingly chaotic as $\kappa\tau$ is increased. In other words, when the laser is switched on it will produce irregular output before settling down to locked amplitude modulated oscillations.

We claim that the sudden transition from the attracting torus to the much larger chaotic attractor at $\kappa\tau \approx 2.556$ is due to a *boundary crisis*.[20] Before a boundary crisis one finds *chaotic transients* associated with what is called a *chaotic saddle*,[20] which collides with a basin boundary at the boundary crisis. Then the chaotic saddle is replaced by the chaotic attractor, which resembles the unstable manifold just prior to the bifurcation. Figure 6 (c) is evidence that we indeed are dealing with a boundary crisis. After the crisis the unstable manifolds accumulate on the chaotic attractor. This is shown in Fig. 7, where we compare the trace of the chaotic attractor for $\kappa\tau = 2.700$ with the 1D unstable manifold of a saddle periodic orbit on the upper part of the branch $\boldsymbol{S}$.

6. CONCLUSIONS

We presented a detailed investigation of a route to chaos via the break-up of a torus in a PCF laser. Our results clearly indicate that the chaotic attractor associated with this transition is created in a boundary crisis. This result was obtained with advanced numerical tools for DDEs, namely the package DDE-BIFTOOL to compute saddle periodic orbits combined with our new technique for computing 1D unstable manifolds of saddle periodic orbits. This highlights the usefulness of these new tools for the study of transitions to chaos in lasers subject to feedback and, more generally, for DDE models arising in applications.

In light of potential uses of chaotic laser output for communication schemes,[12] it is important to make statements about the dimensionality of chaotic attractors in laser systems. From our bifurcation analysis we conclude that the transition to chaos studied here can occur in an ordinary differential equation with a phase space of dimension three. In other words, the chaos that ensues for $\kappa\tau \approx 2.600$ is essentially three-dimensional. Preliminary studies show that chaos in other bubbles may be higher-dimensional. What are the mechanisms involved in routes to higher-dimensional chaos? This is one of the open questions in the bifurcation theory of DDEs. We expect that the techniques described here will contribute to answering this questions.

ACKNOWLEDGMENTS

We thank Koen Engelborghs for his help with DDE-BIFTOOL. B.K. is supported by an EPSRC Advanced Research Fellowship and acknowledges a travel grant from The Royal Society.

REFERENCES

1. G. R. Gray, D. H. DeTienne and G. P. Agrawal, "Mode locking in semiconductor lasers by phase-conjugate optical feedback", *Opt. Lett.* **20**, p. 1295, 1995.
2. G. P. Agrawal and G. R. Gray, "Effect of phase-conjugate feedback on the noise characteristics of semiconductor lasers", *Phys. Rev. A* **46**, p. 5890, 1992.
3. G. H. M. van Tartwijk, H. J. C. van der Linden and D. Lenstra, "Theory of a diode laser with phase-conjugate feedback", *Opt. Lett.* **17**, p. 1590, 1995.
4. G. R. Gray, D. Huang, and G. P. Agrawal, "Chaotic dynamics of semiconductor lasers with phase-conjugate feedback", *Phys. Rev. A* **49**, p. 2096, 1994.
5. B. Krauskopf and D. Lenstra, editors, *Fundamental Issues of Nonlinear Laser Dynamics*, AIP Conference Proceedings **548**, 2000.
6. O. Diekmann, S. A. van Gils, S. M. Verduyn Lunel, H. -O. Walther, *Delay Equations: Functional-, Complex-, and Nonlinear Analysis*, Springer-Verlag, 1995.
7. S. M. Verduyn Lunel and B. Krauskopf, "The mathematics of delay equations with an application to the Lang-Kobayashi equations", in [5], pp. 66–86.
8. A. Gavrielides, "Nonlinear dynamics of semiconductor lasers: Theory and experiments", in [5], pp. 191–217.
9. J. Mørk, B. Tromborg and J. Mark, "Chaos in semiconductor lasers with optical feedback: Theory and experiment", *IEEE J. Quantum Elec.* **28**, p. 93, 1992.
10. T. Heil, I. Fischer, W. Elsässer. J. Mulet and C. R. Mirasso, "Chaos synchronization and spontaneous symmetry-breaking in symmetrically delay-coupled semiconductor lasers", *Phys. Rev. Lett.* **86**, p. 795, 2001.
11. X. S. Yao and L. Maleki, "Dual microwave and optical oscillator", *Opt. Letters* **22**, p. 1867, 1997.
12. G. D. Van Wiggeren and R. Roy, "Communication with chaotic lasers", *Science* **279**, p. 1198, 1998.
13. I. Fischer, Y. Liu and P. Davis, "Synchronization of chaotic semiconductor laser dynamics on subnanosecond time scales and its potential for chaos communication", *Phys. Rev. A* **62**, 011801, 2000.
14. B. Krauskopf, G. R. Gray, and D. Lenstra, "Semiconductor laser with phase-conjugate feedback: Dynamics and bifurcations", *Phys. Rev. E* **58**, p. 7190, 1998.
15. K. Green, B. Krauskopf and K. Engelborghs, "Bistability and boundary crisis in a semiconductor laser with phase-conjugate feedback", preprint (2002), `http://www.enm.bris.ac.uk/research/reports/2002r02.html`
16. B. Krauskopf, G. H. M. van Tartwijk, and G. R. Gray, "Symmetry properties of lasers subject to optical feedback", *Opt. Commun.* **177**, p. 347, 2000.
17. B. Krauskopf and K. Green, "Computing unstable manifolds of periodic orbits in delay differential equations", preprint (2002). `http://www.enm.bris.ac.uk/anm/preprints/2002r01.html`
18. K. Green and B. Krauskopf, "Global bifurcations and bistability at the locking boundaries of a semiconductor laser with phase-conjugate feedback", preprint (2001), `http://www.enm.bris.ac.uk/research/reports/2001r13.html`
19. K. Engelborghs, "DDE-BIFTOOL: a Matlab package for bifurcation analysis of delay differential equations", 2000, `http://www.cs.kuleuven.ac.be/~koen/delay/ddebiftool.shtml`
20. C. Grebogi, E. Ott and J. A. Yorke, "Critical exponent of chaotic transients in nonlinear dynamical systems", *Phys. Rev. Lett.* **57**, p. 11, 1986; C. Grebogi, E. Ott, F. Romeiras and J. A. Yorke, "Critical exponents for crisis-induced intermittency", *Phys. Rev. A* **36**, p. 11, 1987; C. Robert, K. T. Alligood, E. Ott and J. A. Yorke, "Explosions of chaotic sets", *Physica D* **144**, p. 44, 2000.